Taylor & Francis
Taylor & Francis Group

Arctic, Antarctic, and Alpine Research

An Interdisciplinary Journal

ISSN: 1523-0430 (Print) 1938-4246 (Online) Journal homepage: https://www.tandfonline.com/loi/uaar20

Near-Surface Air Temperature Lapse Rate Over Complex Terrain in the Southern Ecuadorian Andes: Implications for Temperature Mapping

Mario Córdova, Rolando Célleri, Cindy J. Shellito, Johanna Orellana-Alvear, Andrés Abril & Galo Carrillo-Rojas

To cite this article: Mario Córdova, Rolando Célleri, Cindy J. Shellito, Johanna Orellana-Alvear, Andrés Abril & Galo Carrillo-Rojas (2016) Near-Surface Air Temperature Lapse Rate Over Complex Terrain in the Southern Ecuadorian Andes: Implications for Temperature Mapping, Arctic, Antarctic, and Alpine Research, 48:4, 673-684, DOI: 10.1657/AAAR0015-077

To link to this article: https://doi.org/10.1657/AAAR0015-077

Published online: 05 Jan 2018.

Arctic, Antarctic, and Alpine Research, Vol. 48, No. 4, 2016, pp. 673–684
DOI: http://dx.doi.org/10.1657/AAAR0015-077

Near-surface air temperature lapse rate over complex terrain in the Southern Ecuadorian Andes: implications for temperature mapping

Mario Córdova[1,*], Rolando Célleri[1,2], Cindy J. Shellito[3], Johanna Orellana-Alvear[1,4,5], Andrés Abril[1], and Galo Carrillo-Rojas[1,4,5]

[1]Departamento de Recursos Hídricos y Ciencias Ambientales, Universidad de Cuenca, Víctor Manuel Albornoz y los Cerezos, Campus Balzay, Cuenca, 010207, Ecuador
[2]Facultad de Ciencias Agropecuarias, Universidad de Cuenca, Avenida 12 de Octubre, Campus Yanuncay, Cuenca, 010205, Ecuador
[3]Department of Earth and Atmospheric Sciences, University of Northern Colorado, Greeley, Colorado 80639, U.S.A.
[4]Facultad de Ciencias Químicas, Universidad de Cuenca, Avenida 12 de Abril y Agustín Cueva, Cuenca, 010203, Ecuador
[5]Laboratory for Climatology and Remote Sensing, Faculty of Geography, University of Marburg, Deutschhausstraße 12, D-35032 Marburg, Germany
[*]Corresponding author's email: marioandrescm89@gmail.com

A B S T R A C T

Near-surface air temperature variation with altitude (Tlr) is important for several applications including hydrology, ecology, climate, and biodiversity. To calculate Tlr accurately, a dense monitoring network over an altitudinal gradient is needed. Typically, meteorological monitoring in mountain regions is scarce and not adequate to calculate Tlr correctly. To overcome this problem in our region, we monitored temperature over a gradient ranging 2600–4200 m a.s.l. during an 18 month period. Using these data, we calculated Tlr for the first time at this altitude in the Andes and tested the impact of using the standard Tlr values instead of the observed ones to map temperature by means of the MTCLIM model. We found that annual lapse rate values (6.9 °C km^{-1} for Tmean, 5.5 °C km^{-1} for Tmin, and 8.8 °C km^{-1} for Tmax) differ significantly from the MTCLIM default values and that temperature maps improved vastly when measured Tlr was entered, especially for Tmax and Tmin. Our results may be representative of the broader area, as Tlr in our study period is not affected by microclimatic conditions generated by differences in topography and land cover between our monitoring sites; moreover, observed temperature during our study period was found to be representative of the longer-term annual climatology of the region.

Introduction

Mountains represent almost 25% of the continental surface (Beniston, 2006), are the home to a quarter of the global population (Meybeck et al., 2011), and directly or indirectly provide sustenance and water for over half of the world inhabitants (Beniston, 2006). In South America, the Andes are the major source of water for the highlands of Venezuela, Colombia, and Ecuador, including much of the adjacent lowland areas and the arid coastal plains of northern Perú (Buytaert et al., 2006). Mountainous ecosystems are complex and fragile and therefore highly susceptible to climate change (Y. Li et al., 2015). In spite of this importance and vulnerability, climate in these ecosystems has been poorly studied because of difficult accessibility of mountain areas, which

has led to a sparse and scarce distribution of high altitude stations (Córdova et al., 2015).

Spatial distribution of temperature is important for numerous applications such as hydrology (Hamlet and Lettenmaier, 2005; Maurer et al., 2002), ecology (Graae et al., 2012; Prentice et al., 1992), surface energy balance models (Arnold et al., 2006), climate modeling (Otto-Bliesner et al., 2006), and remote sensing (Liou and Kar, 2014). Nevertheless, it is difficult to compute it accurately due to the deficiency of the monitoring that is needed to calculate temperature lapse rate (Tlr, temperature variation with altitude), which in turn is useful to determine the spatial distribution of temperature. Typically, observed temperature lapse rate values are not available and Tlr has been assumed to be between 6 and 6.5 °C km^{-1} (Minder et al., 2010; Rolland, 2003; Steenburgh et al., 1997) to calculate spatial distribution of temperature. The use of these values has been commonly justified because they are representative of the theoretical moist adiabatic lapse rate (Hamlet and Lettenmaier, 2005), and also because various sources define middle troposphere saturated lapse rate values within this range (Wallace and Hobbs, 2006). Nonetheless, this assumption has been proven to be erroneous numerous times (Minder et al., 2010; Rolland, 2003; Steenburgh et al., 1997). For instance, several studies have found large annual, seasonal, and diurnal variation of Tlr (Kirchner et al., 2013; Li et al., 2013; Chen et al., 2014; Li et al., 2015). Other studies have reported substantial differences in Tlr for each slope of the same mountain (Minder et al., 2010; Tang and Fang, 2006), which indicates the importance of microclimate for lapse rate. Research in mainland China showed that Tlr varies widely not only temporally but also spatially (Y. Li et al., 2015). Thus, it has been extensively demonstrated that using the theoretical moist adiabatic lapse rate inaccurately reproduces near-surface temperature.

A common approach is to estimate the spatial distribution of temperature by means of extrapolating weather data using a model. Many empirical models have been developed for this purpose, such as the Mountain Microclimate Simulation Model, MTCLIM (Running et al., 1987); the Parameter-elevation Relationships on Independent Slopes Model, PRISM (Daly et al., 1994); the meteorological data preprocessing library MeteoIO (Bavay et al., 2010); and the DAYMET model (Thornton et al., 1997), to name a few. We chose to use MTCLIM because it has been widely applied in mountainous areas where temperature is influenced not only by elevation but also by latitude, longitude, and topography (Almeida and Landsberg, 2003; McCutchan and Fox, 1986; Pietsch and Hasenauer, 2002; Shepherd et al., 2010; Zhao et al., 2005). Furthermore, the source code of MTCLIM is open and it can be modified according to user demand, which we needed in order to test the impact of using the default lapse rate values instead of the measured ones.

A common approach to calculating spatial distribution of temperature is to combine dense monitoring networks with high temporal resolution (Lundquist and Cayan, 2007) and modeling. Therefore, in this study we installed nine temperature sensors in the Andes of South Ecuador ranging 2600–4200 m altitude. Using these data we (1) calculated Tlr and its seasonal variability for the first time at this altitude in the Andes, (2) performed a sensitivity analysis in order to determine if two and three sensors are sufficient to accurately reproduce lapse rate in the study area, and (3) determined if the default MTCLIM values can accurately substitute the observed near-surface lapse rate values to map daily mean, maximum, and minimum temperature.

Materials and Methods

Study Area

The study area is within the *Macizo del Cajas*, declared as part of the World Network of Biosphere Reserves (WNBR) by UNESCO in 2013. *Macizo del Cajas* is a flora endemism center. At least 16 species of vascular plants are unique to the area and 71 species endemic to Ecuador grow in this place (Chacón et al., 2006). There are also two mammal species that are endemic to the Biosphere Reserve (Sánchez and Carbone, 2007), and seven bird species that are endemic to the Andes (Tinoco and Astudillo, 2007). As pointed out by Pepin et al. (2015), these rare species that reside in restricted altitudinal zones within a mountain range are especially vulnerable to climate change, and the consequent change in temperature distribution. This could lead to loss of their habitat because of the continental

insularity effect, which is a powerful driver of biodiversity and endemism in the Tropical High Andes (Anthelme et al., 2014). The study area itself is along an altitudinal gradient located in the eastern side of the Andes, mostly in Cajas National Park. The lowest point is located in the outskirts of the city of Cuenca (2600 m a.s.l.) and the highest one corresponds to one of the highest peaks of the region (4200 m a.s.l.).

Instrumentation

We installed nine temperature sensors along an altitudinal gradient ranging from 2600 to 4200 m a.s.l. (Fig. 1, part A; Table 1). We used two different types of temperature sensors: Campbell Scientific CS215 in six locations, and HOBO Pro v2 in the other three locations (Fig. 1, part A). The CS215 sensors were equipped with the 41303-5A radiation shield, and the Pro v2 with the RS3 solar radiation shield. All of the sensors were installed 2 m above the ground and uniformly distributed in different land cover types within the study area (Fig. 1, part C; Table 1). All sensors were situated well away from any shading effects, including those at sites within or near a forest canopy. For a 6-month period, we installed all of the HOBO sensors together at the Toreadora site to test for accuracy. The measurements from this period were compared to the Campbell CS215 data. Temperature measurements were accurate for all the HOBO sensors (bias < 0.01 °C, $R^2 > 0.99$ for all of the sensors). During our 18-month study period (February 2014–July 2015), temperature was registered every 5 minutes, and those data were used to calculate daily mean, maximum, and minimum temperature. Additionally, to determine if the data from our study period was representative of the climatology of the region we used long-term data (1981–2010) from a nearby weather station (El Labrado), located in another valley approximately 15 km northwest of our study area (3260 m a.s.l., 2°43′58″S, 79°4′23″W) and operated by the Ecuadorian National Institute for Meteorology and Hydrology (INAMHI). We compared these data to the observations from site 6 (which is the closest one in altitude) and found that our study period is representative of the climatology of the region (Fig. 2); moreover, the standard deviation of the long-term data is less than 0.5 °C for every month, which indicates that year-to-year variation is minimal in the region.

Temperature Lapse Rate

To calculate Tlr, we averaged daily values and made two regressions. The first was a multiple linear regression with temperature as the dependent variable and altitude, slope, and aspect as the indepent variables. We also made a simple linear regression between temperature and altitude because we hypothesized that elevation is the main driver of Tlr in our region. We did this for mean, maximum, and minimum temperature and averaged Tlr over annual and monthly scales. We used the first 12 months of data to calculate Tlr and the last 6 months to validate these results for temperature mapping.

Model

To evaluate the impact of using the standard lapse rate values on calculating temperature distribution, we used the mountain microclimate simulation model MTCLIM (Running et al., 1987). The model uses observations of daily maximum temperature, minimum temperature, and precipitation from one location (the base) to estimate daily temperature, precipitation, radiation, and humidity at another location (the target). In this study, we used the model to calculate temperature only; estimates at the target are based on temperature at the base and Tlr.

Tlr default values in the model are 3 °C km^{-1} and 6 °C km^{-1} for minimum and maximum temperature, respectively. MTCLIM does not calculate Tmean, thus we modified the model to compute it and used 6.5 °C km^{-1} as default Tlr, as previously used in several studies (Arnold et al., 2006; Otto-Bliesner et al., 2006; Prentice et al., 1992). We acknowledge that 6 °C km^{-1} is too low for Tmax lapse rate because Tmax is expected to have a steeper lapse rate than Tmean; however, we chose to use this value as it is in the default setup in MTCLIM, thus it has been used in other similar studies where they test this model (Pietsch and Hasenauer, 2002; Shou-zhang et al., 2014).

Temperature Maps

A common practice in calculating temperature at high altitudes is to use temperature data from

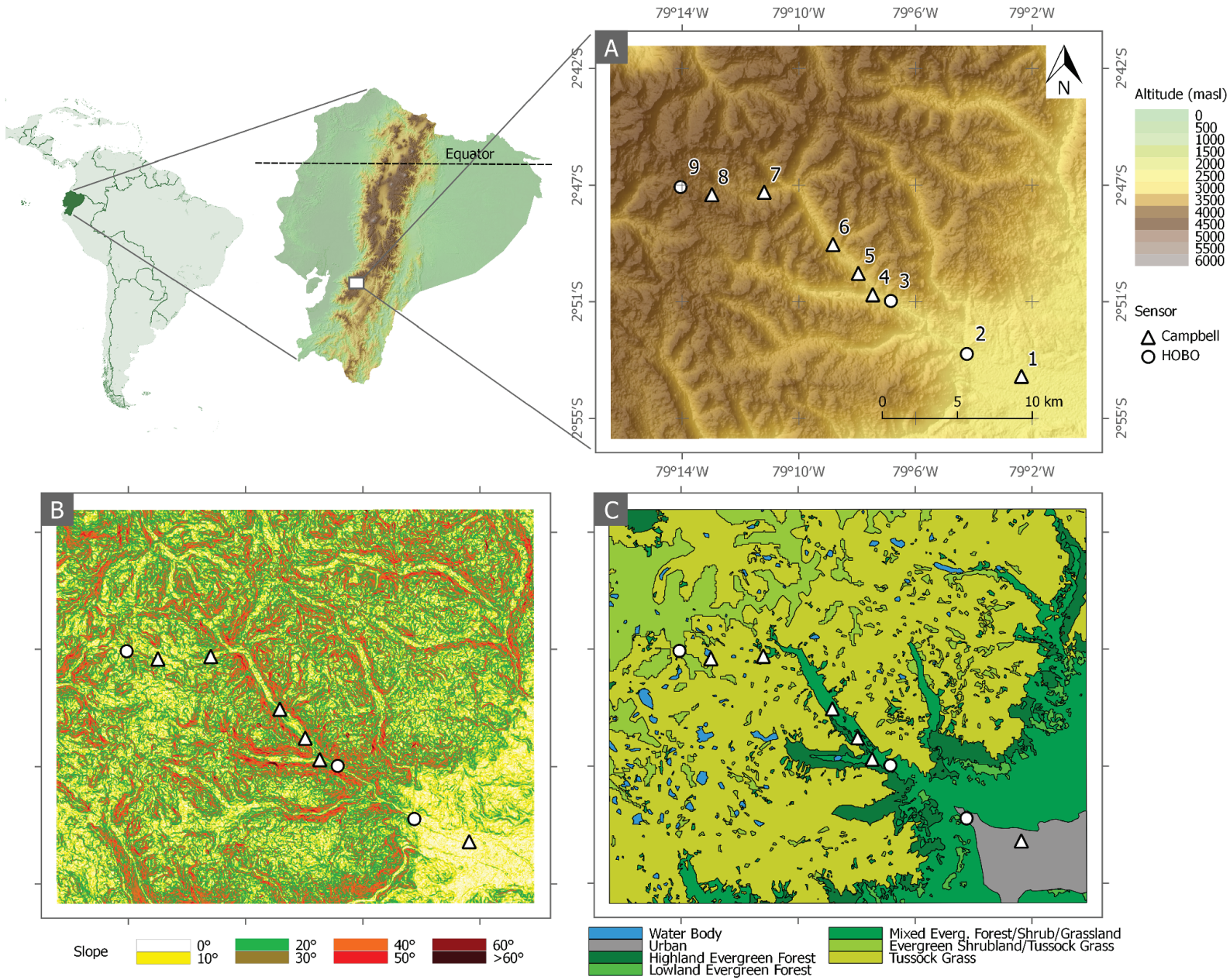

FIGURE 1. (A) Location and elevation of the study area and the sensors of the monitoring network; (B) slope map of the study area; and (C) land cover map of the study area.

TABLE 1

Altitude, coordinates, slope, aspect, and land cover of the sites where the sensors used in the present study were installed.

Sensor	Station	Altitude (m)	Longitude (°)	Latitude (°)	Slope (°)	Aspect (°)	Land cover
1	Balzay	2610	–79.000	–2.879	0	—	Urban
2	Sayausí	2712	–79.069	–2.879	4.7	61.7	Urban
3	Llaviuco	3045	–79.126	–2.843	6.0	–177.0	Forest/Shrubland
4	OPNC	3060	–79.115	–2.847	13.2	19.3	Forest
5	Matadero	3209	–79.134	–2.831	1.6	90.0	Forest
6	Chirimachay	3298	–79.150	–2.813	12.0	42.9	Forest/Shrubland
7	Virgen	3626	–79.191	–2.782	7.2	118.8	Tussock Grass
8	Toreadora	3955	–79.222	–2.783	4.5	–77.9	Tussock Grass
9	Tres Cruces	4200	–79.241	–2.779	11.1	175.1	Tussock Grass

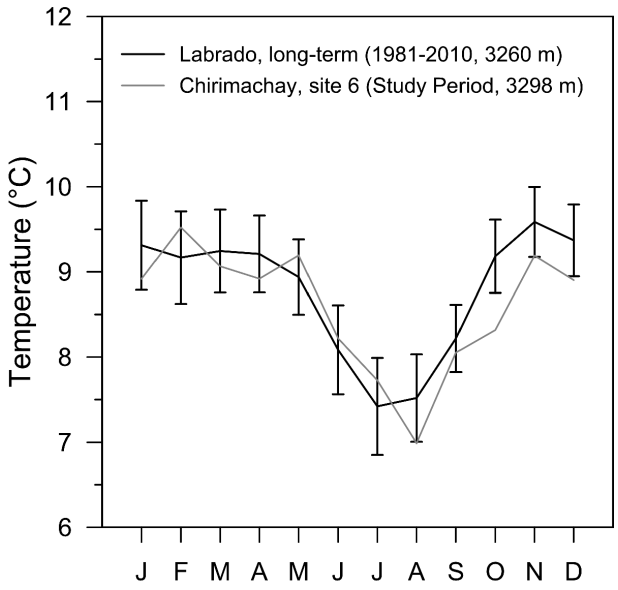

FIGURE 2. Long-term monthly mean temperature from a nearby weather station (black line, the error bars show the standard deviation for the 1981–2010 period) compared to data from the closest station in elevation (site 6) used in the present study (gray line).

a station in the valley bottom (the base) and extrapolate upland temperature (the target) using a standard lapse rate value (Komatsu et al., 2010; Y. Li et al., 2015; Tang and Fang, 2006). Therefore, in the model we used daily temperature data from the lowest sensor (sensor 1) as input to extrapolate temperature to the higher altitudes in a digital elevation model (Aster GDEM v2, with 30 m resolution) (LP DAAC, 2011; Tachikawa et al., 2011). We performed four analyses using this methodology and MTCLIM.

First, we calculated temperature distribution in the study area using the default lapse rate values of MTCLIM: 3 and 6 °C km^{-1} for minimum and maximum temperature, respectively, and the commonly used lapse rate value (6.5 °C km^{-1}) for mean temperature. We did this because it is the common approach used when there is no temperature data to calculate Tlr. Next, we used observed annual average Tlr to calculate temperature distribution in the study area.

Then, we calculated Tlr separately for each season in order to test if this procedure improves temperature distribution calculations. Further details on Tlr seasonality in the study area will be given in the results and discussion section. And finally, we calculated annual Tlr using only two (1 and 9) and three (1, 6, and 9) sensors. We used these sensors' data to calculate temperature distribution in order to determine how dense a monitoring network in the study area should be.

To evaluate the model performance, we compared the simulated values that correspond to the pixel where each sensor is located to the actual observations for the corresponding day. Additionally, to evaluate the ability of the model to predict upland temperature we used the observed Tlr (which was calculated for the first 12 months) to calculate and validate spatial temperature distribution for the last 6 months of our data set. Finally, we calculated mean bias error (MBE), mean absolute error (MAE), and root mean square error (RMSE) for sensors 2 to 9 for the study period.

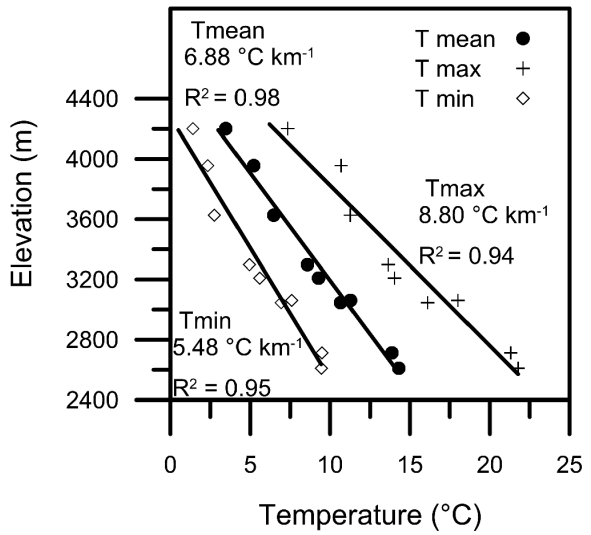

FIGURE 3. Temperature and elevation linear regression for Tmean, Tmax, and Tmin, and Tlr annual values.

Results and Discussion

Annual, Monthly, and Seasonal Lapse Rate

The multiple linear regression resulted in p-values of 0.86 for slope, 0.93 for aspect, and a value of less than 0.001 for elevation. Based on these results, we decided to calculate Tlr using a simple linear regression between temperature and elevation, as this variable clearly is the major temperature driver in our study area. Figure 3 shows the linear regressions in altitude for mean, maximum, and minimum temperature for the study period. As expected, the lapse rate is steepest for maximum temperature (8.80 °C km^{-1}), and less steep for mean (6.88 °C km^{-1}) and minimum temperature (5.48 °C km^{-1}). The differences in the slopes of these lines are due to the greater fluctuation in the diurnal temperature cycle at lower elevations as reflected in other studies (Tang and Fang, 2006; Yoshino, 1975). The annual average diurnal temperature range (DTR) for our study site varied from 12.5 °C at 2600 m a.s.l. to 6 °C at 4200 m a.s.l. One factor that may influence the DTR is the relative position of a station with respect to local topography. For example, at a station located in a protected mountain valley, the DTR may be high due to the formation of a stable nocturnal boundary layer, while at a station located on a hilltop or at a high altitude location, DTR may be low because exposure to the free atmosphere keeps nocturnal conditions less cold. To ascertain whether this is a factor at our stations, we analyzed DTR values using wind speed as a proxy for boundary layer conditions: for well-mixed days (daily wind speed > 5 m s^{-1} [Oke, 2002]), and calm days (daily wind speed < 1 m s^{-1}). To categorize well-mixed and calm days, we used wind speed data from site number 8 (3955 m a.s.l.) because it is the only site where daily wind speed reaches values higher than 5 m s^{-1}; additionally, these were also the windiest (and less windy) days at the lowest elevation and they can be used to analyze well-mixed and calm conditions. We found that DTR at the lowest station was 12.61 °C and 12.79 °C for calm and well-mixed days, respectively; similarly, DTR for site number 8 was 7.37 °C and 7.68 °C for calm and well-mixed days, respectively. Therefore, DTR differences with elevation may not be associated with boundary layer microclimates generated by topographical variations. To confirm this hypothesis, specific research is encouraged (i.e., atmospheric soundings for better data on boundary layer conditions). In addition, the higher elevations are more persistently cloudy or foggy, which reduces the diurnal temperature variations. For example, annual average relative humidity is around 80% at the lower stations, but it is higher than 95% at the higher elevations. Furthermore, annual average solar radiation is 14.5 MJ m^{-2} d^{-1} at the lowest elevation compared to 11.35 MJ m^{-2} d^{-1} at site number 8 even though clear sky solar radiation is greater at the higher elevations. This persistent near-saturation and cloudier state has the effect of moderating daily fluctuations in temperature at the higher stations. The variation in the lapse rate between Tmax and Tmin also reflects changes in atmospheric stability through the diurnal cycle. There is reduced stability during the day, with more heating at lower elevations, and more stability at night, with more rapid cooling at the lower elevations—especially on nights with lower relative humidity or reduced cloud cover, both of which are more common conditions at the lower altitudes as relative humidity and solar radiation data suggest.

In addition to finding differences between standard and observed lapse rate, previous studies have

found large subannual variations of Tlr (Chen et al., 2014; Kirchner et al., 2013; X. Li et al., 2013; Y. Li et al., 2015). To identify subannual Tlr variation in our study site, we calculated monthly Tlr for mean, maximum, and minimum temperature. Figure 4 shows a small change in lapse rate for mean temperature throughout the year (approximately 0.5 °C km^{-1}); it peaks in July through August, and again in December through February. The same pattern is reproduced in the small peak for Tmin lapse rate in August and the peak in Tmax lapse rate in December through February. This small-amplitude cycle reflects the temperature fluctuations associated with precipitation seasonality, which follows a bimodal pattern with a maximum in March through May, and another small peak in September through November (Fig. 4). The precipitation average showed in Figure 4 was calculated using data from five sites within our study area. Although precipitation amount varies with altitude, the pattern is the same throughout the gradient; hence, the data shown in Figure 4 is valid for identifying rainfall seasonality in the study area. These results are in agreement with the patterns found by Célleri et al. (2007) using long-term precipitation data in the region.

In addition to the precipitation seasonality, substantial differences are found in other variables for the wet and the dry seasons at the lower and the higher elevations, as highlighted in Table 2. Solar radiation is more variable at the lowest altitudes; it diminishes by 10% in the wet season compared to the dry season average, whereas it diminishes by only 5% at the higher altitudes. This variability is also reflected on relative humidity data that remain constant throughout the year at the highest altitudes, but it shows seasonality at the lower elevations. Precipitation shows the most remarkable altitudinal differences: in the dry season the rainfall amount is about 32% less at the low altitudes compared to the highlands, whereas this amount is 7% higher in the lower elevations during the wet season. In summary, the data in Table 2 suggest that lapse rates are lower in the wet periods because these periods have a greater impact on temperature at lower elevations through reduced solar radiation. This causes the diurnal temperature range to narrow during these times of the year.

In order to determine if the identified mean temperature seasonal lapse rate differences are statistically significant, we performed a nonparametric randomization test for comparing the means of the Tlr for the dry and wet seasons. First, we determined the mean Tlr difference between the dry (JJA, DJF) and the wet (MAM, SON) seasons (see abbreviation definitions below). Then we calculated the mean difference between every possible combination of six-month averages and the average

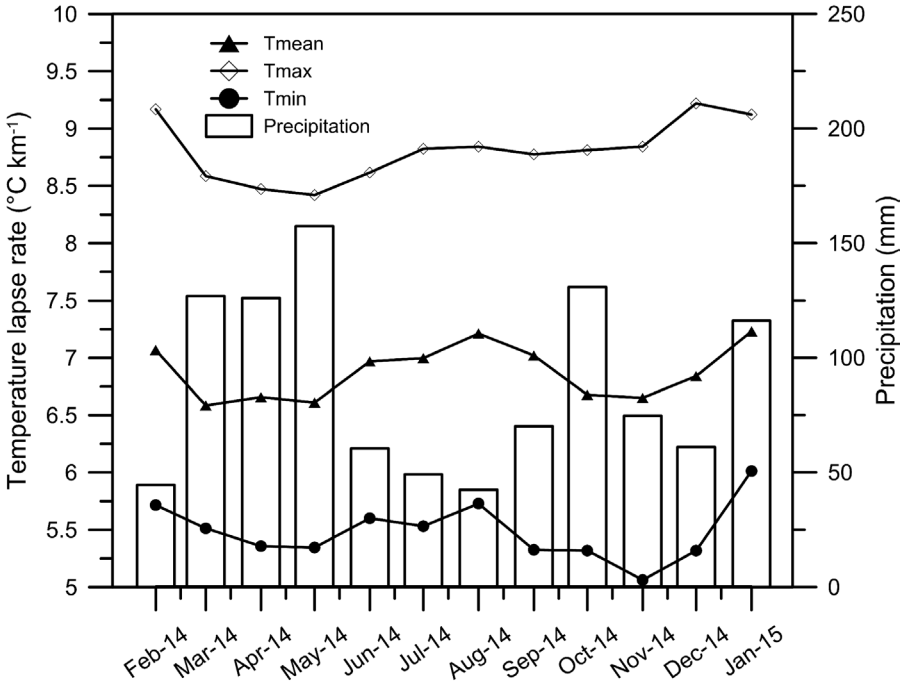

FIGURE 4. Monthly Tlr for Tmean, Tmax, and Tmin and monthly average precipitation in the gradient. The precipitation average was calculated from tipping bucket rain gauges located at sites 1, 4, 6, 7, and 8.

TABLE 2

Average solar radiation, relative humidity, and precipitation for the dry (JJA, DJF) and the wet (MAM, SON) seasons. Average values calculated for the lowest (site 1) and the highest (site 8) sites where all these variables were measured.

Site	Season	Solar radiation (MJ m^{-2} day^{-1})	Relative humidity (%)	Precipitation (mm)
1	dry	14.5	76	297
	wet	13.0	82	672
8	dry	11.1	93	435
	wet	10.5	93	630

of the remaining six months. The difference of the medians between the observed dry and wet seasons was –0.353 °C and occupied the 0.43 percentile in the resulting distribution; therefore, we can conclude that Tlr for Tmean is significantly different for dry and wet conditions. The presence of this marked seasonal pattern in our study area prompted us to calculate seasonal average Tlr to determine if it improves temperature mapping. We divided the one-year study period into four seasons: December-January-February (DJF), March-April-May (MAM), June-July-August (JJA), and September-October-November (SON); seasonal Tlr values are shown in Table 3. Although seasonality exists and is more evident for Tmean lapse rate, the variation is not as wide as that found in the mid-latitudes (Minder et al., 2010; Kirchner et al., 2013; Li et al., 2015). The amplitude of seasonal variation in the mid-latitudes is due to greater seasonal variation in temperature, overall, where the presence of warmer air masses in summer increases lapse rate, while cool, dry air masses in winter tend to decrease lapse rate (Blandford et al., 2008).

TABLE 3

Seasonal Tlr values for Tmean, Tmax, and Tmin.

Season	Tlr (°C Km^{-1}) Max	Mean	Min
DJF	9.17	7.05	5.68
MAM	8.49	6.62	5.41
JJA	8.76	7.06	5.62
SON	8.81	6.78	5.24

Sensitivity Analysis

Figure 3 shows that all the points are near the regression lines, especially for mean temperature. This indicates that a simpler monitoring network could be sufficient to calculate Tlr correctly in our study area. In order to test this hypothesis, we calculated Tlr using two sensors only (1 and 9), and three sensors only (1, 6, and 9). Table 4 shows that the Tlr values when only two and three monitoring points were used for its calculation are not significantly different than the ones obtained using all nine sensors. Furthermore, the fact that sites 1, 6, and 9 are in urban, forest/shrubland, and tussock grass areas, respectively, evidences that near-surface air temperature and consequently Tlr values are dominated by elevation rather than by land cover characteristics. Therefore, it may be possible to install simpler networks with less monitoring sites—even independent of their land cover, provided that they are free from shading effects—in the region to satisfactorily calculate Tlr. The validity of this hypothesis should be tested in other locations within the region.

Temperature Maps

We mapped maximum, mean, and minimum temperature using MTCLIM and five different lapse rates: MTCLIM default (for Tmax and Tmin) and the commonly used lapse rate (for Tmean), annual, seasonal, two points only, and three points only. Figure 5 shows MAE at four stations uniformly distributed in the gradient for the validation period (February 2015–July 2015). Error is considerably lower for mean temperature; this is because standard Tlr for mean temperature is close to the observed Tlr. For Tmax and Tmin, higher errors were observed, and MAE was always the highest when default MTCLIM Tlr values were used. For Tmax,

TABLE 4

Tlr values calculated using two and three sensors compared to the Tlr calculated using all the nine sensors of the network.

Number of sensors used	Tlr (°C Km^{-1}) Max	Mean	Min
2	9.08	6.82	5.06
3	8.98	6.76	5.00
9	8.80	6.88	5.48

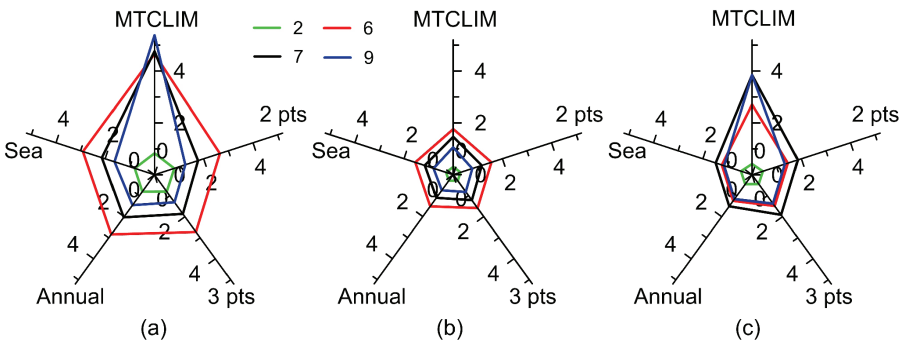

FIGURE 5. Mean absolute error (°C) of the temperature maps using different lapse rates (MTCLIM: default MTCLIM values; Sea: seasonal lapse rate values; 2 pts: annual lapse rate calculated with two sensors; 3 pts: annual lapse rate calculated with three sensors only; Annual: annual observed lapse rate) at four sites distributed uniformly along the gradient. (a) Maximum temperature, (b) mean temperature, and (c) minimum temperature.

errors were the highest and they were almost equal for annual, seasonal, two points, and three points Tlr maps; whereas for Tmin, errors were slightly lower for seasonal and annual Tlr maps. In general, highland temperature calculations degraded as the target elevation increased.

The analysis of the results obtained with the different Tlr values suggests that for this case, the most effective way to map daily temperature was to use annual Tlr because it is simpler for modeling and the results were as accurate as the ones obtained when we used seasonal Tlr. Figure 6 shows daily tempera-

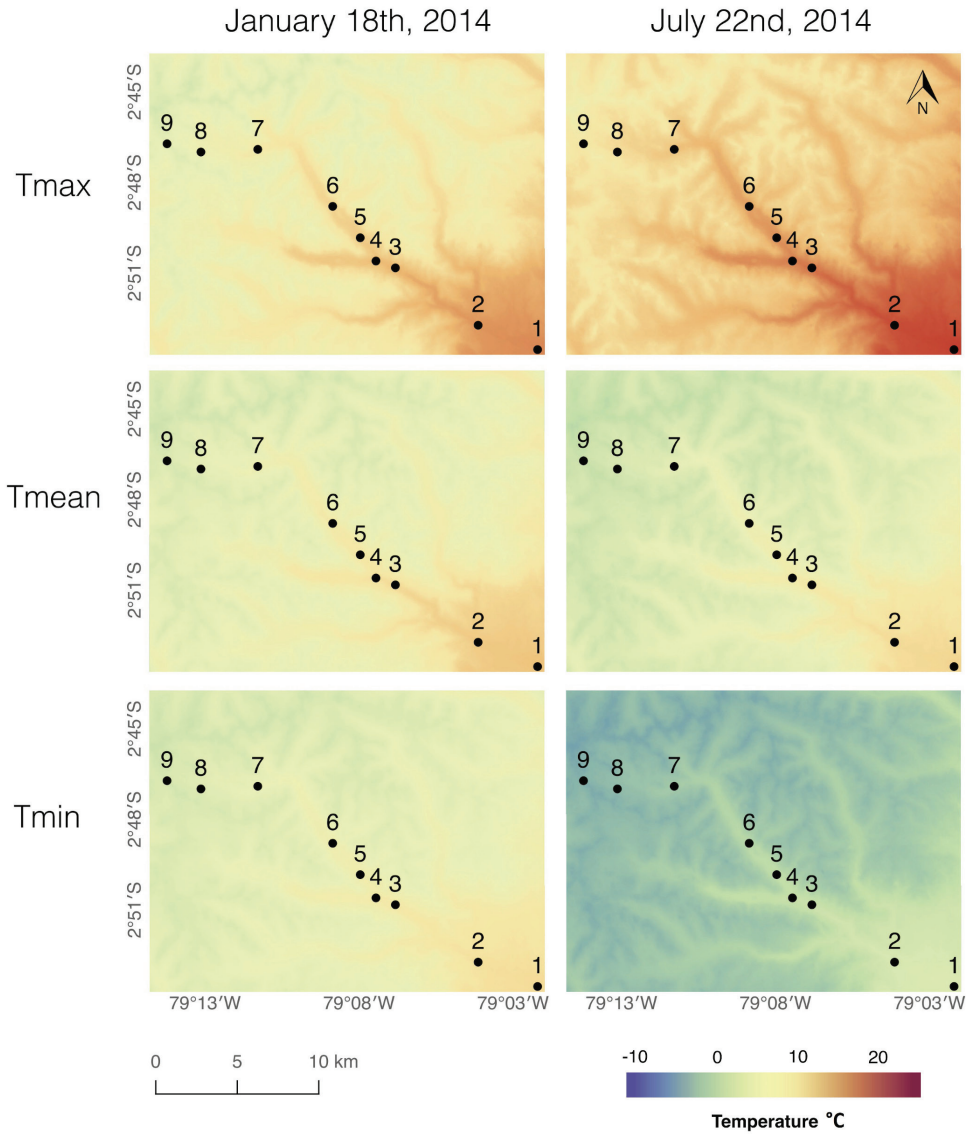

FIGURE 6. Temperature maps of the study area calculated using annual Tlr for two representative days, one of a wet period (18 January), and one of a dry period (22 July).

ture mapped using annual Tlr and MTCLIM for two representative days in the study area, one of a wet period (18 January 2014) and and one of a dry period (22 July 2014). Cloudier skies in the MAM rainy season cause the diurnal temperature range not to be as large as in the JJA dry season, as also found by Fries et al. (2009) in a tropical mountain forest ecosystem of Southern Ecuador in a gradient ranging from 1950 to 2993 m a.s.l. During the dry season, clear skies cause maximum temperature to be warmer at midday, and minimum temperature to be lower before sunrise as more outgoing longwave radiation escapes through the atmosphere without clouds to emit it back to the surface.

Conclusions

The main goal of the current study was to determine if standard lapse rate values can be used to substitute for the observed near-surface temperature lapse rate accurately in the Andes of Southern Ecuador, in an area spanning from the inter-Andean valley in the outskirts of the city of Cuenca to the *páramo* ecosystem in the Macizo del Cajas Biosphere Reserve. In this region, high-density climate monitoring is extremely scarce; therefore, it is of utmost importance to gain knowledge on the validity of the use of standard atmospheric lapse rate values for different applications. To this end, we calculated Tlr for Tmean, Tmax, and Tmin using a one-year period from a unique monitoring network (nine sensors ranging 2600 to 4200 m a.s.l.) and used these values to test how they improve the calculation of spatial distribution of temperature using the MTCLIM model.

We identified that observed mean temperature lapse rate (6.88 °C km^{-1}) is close to the commonly used lapse rate (6.5 °C km^{-1}); however, we should investigate further implications of this apparently small difference in Tmean lapse rate (e.g., impact on calculation of other spatial variables related to temperature). In contrast, we found that Tlr values for Tmax and Tmin were very different than the MTCLIM default values, and for this reason, Tmax and Tmin observations along the gradient are extremely important to reproduce upland temperature conditions. The differences found in the slopes of these lapse rates are mainly because of greater diurnal temperature fluctuations at lower elevations caused by cloudier, foggier, and more humid conditions at higher altitudes.

The second major finding was that for this landscape, temperature maps were accurate when only two and three sensors were used to calculate Tlr; these findings suggest that in general, such a dense network would not be required in order to calculate spatial distribution of temperature correctly in the region. A simpler monitoring network would be cheaper to install, maintain, and operate, and it could be implemented regionally to improve operational studies that require these kind of spatial data. Additionally, we analyzed if factors other than elevation affect the observed lapse rate values, and found that topography (e.g., slope and aspect), land cover, and atmospheric stability do not control temperature differences in the gradient; this may indicate that the results found in the present study could be representative of the broader region.

The fine scale and more precise maps obtained in this study will contribute to ongoing and future research in the area as several research projects in multiple disciplines such as hydrology, ecology, ecohydrology, forestry, climate, meteorology, and remote sensing are currently running in the Macizo del Cajas Biosphere Reserve. Moreover, this study and the monitoring network will contribute to expanding our knowledge on mountain climates, as a better understanding of mountain lapse rates and their drivers is fundamental for further improving climatological temperature analysis in high-elevation regions as pointed out by (Minder et al., 2010).

Acknowledgments

This research was carried out under the project "Meteorological cycles and evapotranspiration along an altitudinal gradient in Cajas National Park" funded by Empresa Pública Municipal de Telecomunicaciones, Agua Potable, Alcantarillado y Saneamiento (ETAPA EP-Parque Nacional Cajas) and Dirección de Investigación de la Universidad de Cuenca (DIUC). We are thankful to Secretaría Nacional de Ciencia y Tecnología (SENESCYT) for funding the equipment used in this study, Ministerio del Ambiente del Ecuador (MAE) for the research permissions, and Fundación Jardín del Cajas for providing space within their installations for one of the study sites. We are grateful to the Ecua-

dorian Fulbright Commission for providing support for Cindy J. Shellito. We are also thankful to INAMHI for providing the long-term data. Special thanks are due to the staff and students who contributed to the meteorological monitoring. We also acknowledge the three anonymous reviewers and the associate editor who contributed to greatly improve the quality of the manuscript.

References Cited

Almeida, A. C., and Landsberg, J. J., 2003: Evaluating methods of estimating global radiation and vapor pressure deficit using a dense network of automatic weather stations in coastal Brazil. *Agricultural and Forest Meteorology*, 118(3–4): 237–250. doi http://doi.org/10.1016/S0168-1923(03)00122-9.

Anthelme, F., Jacobsen, D., Macek, P., Meneses, R. I., Moret, P., and Beck, S., 2014: Biodiversity patterns and continental insularity in the tropical High Andes. *Arctic, Antarctic, and Alpine Research*, 46(4): 811–828.

Arnold, N. S., Rees, W. G., Hodson, A. J., and Kohler, J., 2006: Topographic controls on the surface energy balance of a High Arctic valley glacier. *Journal of Geophysical Research: Earth Surface*, 111(F02011): 15.

Bavay, M., Egger, T., and Winkler, L., 2010: MeteoIO: A meteorological data pre-processing library for numerical models. *EGU General Assembly 2010*.

Beniston, M., 2006: Mountain weather and climate: a general overview and a focus on climatic change in the Alps. *Hydrobiologia*, 562(1): 3–16. doi http://doi.org/10.1007/s10750-005-1802-0.

Blandford, T. R., Humes, K. S., Harshburger, B. J., Moore, B. C., Walden, V. P., and Ye, H., 2008: Seasonal and synoptic variations in near-surface air temperature lapse rates in a mountainous basin. *Journal of Applied Meteorology and Climatology*, 47(1): 249–261. doi http://doi.org/10.1175/2007JAMC1565.1.

Buytaert, W., Célleri, R., De Bièvre, B., Cisneros, F., Wyseure, G., Decker, J., and Hofstede, R., 2006: Human impact on the hydrology of the Andean páramos. *Earth-Science Reviews*, 79(1–2): 53–72. doi http://doi.org/10.1016/j.earscirev.2006.06.002.

Célleri, R., Willems, P., Buytaert, W., and Feyen, J., 2007: Space–time rainfall variability in the Paute Basin, Ecuadorian Andes. *Hydrological Processes*, 3327(August): 3316–3327. doi http://doi.org/10.1002/hyp.

Chacón, G., Martínez, J., Tinoco, B., Arbeláez, E., Minga, D., and Zárate, D., 2006: Actualizacion de la Informacion del Componente Biótico del Borrador del Expediente del Parque Nacional Cajas para la Declaratoria de Patrimonio Mundial. Cuenca, Ecuador.

Chen, R., Song, Y., Kang, E., Han, C., Liu, J., Yang, Y., Qing, W., and Liu, Z., 2014: A cryosphere-hydrology observation system in a small alpine watershed in the Qilian Mountains of China and Its meteorological gradient. *Arctic, Antarctic, and Alpine Research*, 46(2): 505–523.

Córdova, M., Carrillo-Rojas, G., Crespo, P., Wilcox, B., and Célleri, R., 2015: Evaluation of the Penman-Monteith (FAO 56 PM) method for calculating reference evapotranspiration using limited data. Application to the Wet Páramo of Southern Ecuador. *Mountain Research and Development*, 35(3): 230–239.

Daly, C., Neilson, R. P., and Phillips, D. L., 1994: A statistical-topographic model for mapping climatological precipitation over mountainous terrain. *Journal of Applied Meteorology*, 33(2): 140–158. doi http://doi.org/10.1175/1520-0450(1994)033<0140:ASTMFM>2.0.CO;2.

Fries, A., Rollenbeck, R., Göttlicher, D., Nauß, T., Homeier, J., Peters, T., and Bendix, J., 2009: Thermal structure of a megadiverse Andean mountain ecosystem in southern Ecuador and its regionalization. *Erdkunde*, 63(4): 321–335. doi http://doi.org/10.3112/erdkunde.2009.04.03.

Graae, B. J., De Frenne, P., Kolb, A., Brunet, J., Chabrerie, O., Verheyen, K., Pepin, N., Heinken, T., Zobel, M., Shevtsova, A., Nijs, I., and Milbau, A., 2012: On the use of weather data in ecological studies along altitudinal and latitudinal gradients. *Oikos*, 121(1): 3–19. doi http://doi.org/10.1111/j.1600-0706.2011.19694.x.

Hamlet, A. F., and Lettenmaier, D. P., 2005: Production of temporally consistent gridded precipitation and temperature fields for the continental United States. *Journal of Hydrometeorology*, 6(3): 330–336. doi http://doi.org/10.1175/JHM420.1.

Kirchner, M., Faus-Kessler, T., Jakobi, G., Leuchner, M., Ries, L., Scheel, H.-E., and Suppan, P., 2013: Altitudinal temperature lapse rates in an Alpine valley: trends and the influence of season and weather patterns. *International Journal of Climatology*, 33(3): 539–555. doi http://doi.org/10.1002/joc.3444.

Komatsu, H., Hashimoto, H., Kume, T., Tanaka, N., Yoshifuji, N., Otsuki, K., Suzuki, M., and Kumagai, T., 2010: Modeling seasonal changes in the temperature lapse rate in a northern Thailand mountainous area. *Journal of Applied Meteorology and Climatology*, 49(6): 1233–1246. doi http://doi.org/10.1175/2010JAMC2297.1.

Li, X., Wang, L., Chen, D., Yang, K., Xue, B., and Sun, L., 2013: Near-surface air temperature lapse rates in the mainland China during 1962–2011. *Journal of Geophysical Research: Atmospheres*, 118(14): 7505–7515. doi http://doi.org/10.1002/jgrd.50553.

Li, Y., Zeng, Z., Zhao, L., and Piao, S., 2015: Spatial patterns of climatological temperature lapse rate in mainland China: a multi-time scale investigation. *Journal of Geophysical Research: Atmospheres*, . doi http://doi.org/10.1002/2014JD022978. Received

Liou, Y. A., and Kar, S. K., 2014: Evapotranspiration estimation with remote sensing and various surface energy balance algorithms—a review. *Energies*, 7(5): 2821–2849. doi http://doi.org/10.3390/en7052821.

LP DAAC. 2011: ASTER GDEM v2. NASA Land Processes Distributed Active Archive Center, USGS/Earth Resources Observation and Science (EROS) Center, Sioux Falls, South Dakota. Retrieved from http://gdex.cr.usgs.gov/gdex.

Lundquist, J. D., and Cayan, D. R., 2007: Surface temperature patterns in complex terrain: daily variations and long-term change in the central Sierra Nevada, California. *Journal of Geophysical Research*, 112(D11): D11124. doi http://doi.org/10.1029/2006JD007561.

Maurer, E. P., Wood, A. W., Adam, J. C., and Lettenmaier, D. P., 2002: A long-term hydrologically based dataset of land surface fluxes and states for the conterminous United States. *Journal of Climate*, 15(22): 3237–3251. doi http://doi.org/10.1175/JCLI-D-12-00508.1.

McCutchan, M. H., and Fox, D. G., 1986: Effect of elevation and aspect on wind, temperature and humidity. *Journal of Climate and Applied Meteorology*, 25(12): 1996–2013.

Meybeck, M., Green, P., and Vörösmarty, C., 2011: A new typology for mountains and other relief classes: an application to global continental water resources and population distribution. *Mountain Research and Development*, 21(1): 34–45.

Minder, J. R., Mote, P. W., and Lundquist, J. D., 2010: Surface temperature lapse rates over complex terrain: lessons from the Cascade Mountains. *Journal of Geophysical Research*, 115(D14122): 13.

Oke, T. R., 2002: *Boundary Layer Climates*. Second edition. London and New York: Routledge, 464 pp.

Otto-Bliesner, B. L., Marshall, S. J., Overpeck, J. T., Miller, G. H., and Hu, A., 2006: Simulating Arctic climate warmth and icefield retreat in the last interglaciation. *Science*, 311(5768): 1751–1753. doi http://doi.org/10.1126/science.1120808.

Pepin, N., Bradley, R. S., Diaz, H. F., Baraer, M., Caceres, E. B., Forsythe, N., Fowler, H., Greenwood, G., Hashmi, M. Z., Liu, X. D., Miller, J. R., Ning, L., Ohmura, A., Palazzi, E., Rangwala, I., Schöner, W., Severskiy, I., Shahgedanova, M., Wang, M. B., Williamson, S. N., and Yang, D. Q. 2015: Elevation-dependent warming in mountain regions of the world. *Nature Climate Change*, 5(5): 424–430. doi http://doi.org/10.1038/nclimate2563.

Pietsch, S. A., and Hasenauer, H., 2002: Using mechanistic modeling within forest ecosystem restoration. *Forest Ecology and Management*, 159(1–2): 111–131. doi http://doi.org/10.1016/S0378-1127(01)00714-9.

Prentice, I. C., Cramer, W., Harrison, S. P., Leemans, R., Monserud, R. A., and Solomon, A. M. 1992: Special paper: a global biome model based on plant physiology and dominance, soil properties and climate. *Journal of Biogeography*, 19(2): 117. doi http://doi.org/10.2307/2845499.

Rolland, C., 2003: Spatial and seasonal variations of air temperature lapse rates in Alpine regions. *Journal of Climate*, 16(7): 1032–1046.

Running, S. W., Nemani, R. R., and Hungerford, R. D., 1987: Extrapolation of synoptic meteorological data in mountainous terrain and its use for simulating forest evapotranspiration and photosynthesis. *Canadian Journal of Forest Research*, 17(6): 472–483. doi http://doi.org/10.1139/x87-081.

Sánchez, F., and Carbone, M., 2007: Guía de mamíferos del Parque Nacional Cajas. Cuenca, Ecuador: ETAPA.

Shepherd, A., Gill, K. M., and Rood, S. B., 2010: Climate change and future flows of Rocky Mountain rivers: converging forecasts from empirical trend projection and down-scaled global circulation modelling. *Hydrological Processes*, 24(26): 3864–3877. doi http://doi.org/10.1002/hyp.7818

Shou-zhang, P., Chuan-yan, Z., Xiao-ping, W., Zhong-lin, X., Xing-ming, L., Hu, H., and Shi-fei, Y., 2014: Mapping daily temperature and precipitation in the Qilian Mountains of northwest China. *Journal of Mountain Science*, 11(4): 896–905. doi http://doi.org/10.1007/s11629-013-2613-9

Steenburgh, W. J., Mass, C. F., and Ferguson, S. A., 1997: The influence of terrain-induced circulations on wintertime temperature and snow level in the Washington Cascades. *Weather and Forecasting*, 12(2): 208–227.

Tachikawa, T., Kaku, M., Iwasaki, A., Gesch, D., Oimoen, M., Zhang, Z., Danielson, J., Krieger, T., Curtis, B., and Haase, J., 2011: *ASTER Global Digital Elevation Model Version 2—Summary of Validation Results,* 31 August 2011. Pasadena, California: Jet Propulsion Laboratory.

Tang, Z., and Fang, J., 2006: Temperature variation along the northern and southern slopes of Mt. Taibai, China. *Agricultural and Forest Meteorology*, 139(3–4): 200–207. doi http://doi.org/10.1016/j.agrformet.2006.07.001.

Thornton, P. E., Running, S. W., and White, M. A., 1997: Generating surfaces of daily meteorological variables over large regions of complex terrain. *Journal of Hydrology*, 190(3–4): 214–251. doi http://doi.org/10.1016/S0022-1694(96)03128-9.

Tinoco, B., and Astudillo, P., 2007: Guía de campo para la obseración de aves del Parque Nacional Cajas. Cuenca, Ecuador: ETAPA.

Wallace, J. M., and Hobbs, P. V., 2006: *Atmospheric Science: An Introductory Survey.* Second edition. Burlington, Massachusetts: Academic Press.

Yoshino, M., 1975: *Climate in a Small Area*. Tokyo: University of Tokyo Press.

Zhao, C., Nan, Z., and Cheng, G., 2005: Methods for modelling of temporal and spatial distribution of air temperature at landscape scale in the southern Qilian mountains, China. *Ecological Modelling*, 189(1–2): 209–220. doi http://doi.org/10.1016/j.ecolmodel.2005.03.016.

MS submitted 3 December 2015
MS accepted 29 August 2016